Available online at www.sciencedirect.com

SCIENCE DIRECT

Biochimica et Biophysica Acta 1706 (2005) 68–80

BIOCHIMICA ET BIOPHYSICA ACTA BBA

http://www.elsevier.com/locate/bba

# Evidence for the role of the oxygen-evolving manganese complex in photoinhibition of Photosystem II

Marja Hakala, Ilona Tuominen, Mika Keränen, Taina Tyystjärvi, Esa Tyystjärvi*

*Department of Biology, Laboratory of Plant Physiology and Molecular Biology, Biocity A, University of Turku, FI-20014 University of Turku, Finland*

Received 6 July 2004; accepted 1 September 2004
Available online 16 September 2004

**Abstract**

Photoinhibition of PSII occurs at the same quantum efficiency from very low to very high light, which raises a question about how important is the rate of photosynthetic electron transfer in photoinhibition. We modulated electron transfer rate and light intensity independently of each other in lincomycin-treated pea leaves and in isolated thylakoids, in order to elucidate the specific effects of light and PSII electron transport on photoinhibition. Major changes in the rate of electron transport caused only small changes in the rate of photoinhibition, suggesting the existence of a significant photoinhibitory pathway that contains an electron-transfer-independent phase. We compared the action spectrum of photoinhibition with absorption spectra of PSII components that could function as photoreceptors of the electron-transfer-independent phase of photoinhibition and found that the absorption spectra of Mn(III) and Mn(IV) compounds resemble the action spectrum of photoinhibition, showing a steep decrease from UV-C to blue light and a low visible-light tail. Our results show that the release of a Mn ion to the thylakoid lumen is the earliest detectable step of both UV- and visible-light-induced photoinhibition. After Mn release from the oxygen-evolving complex, oxidative damage to the PSII reaction center occurs because the Mn-depleted oxygen-evolving complex cannot reduce $P_{680}^{+}$ normally.


*Keywords:* Photoinhibition; Photosystem II; Manganese; Action spectrum

## 1. Introduction

Photosynthesis is a light-driven reaction, but light also damages the photosynthetic machinery. The light-induced damage to the oxygen-evolving PSII is termed photoinhibition and the damaged PSII reaction centers are repaired via de novo synthesis of the D1 protein of PSII core (for reviews, see [1–4]).

Four main hypotheses have been put forward to explain photoinhibition under visible light. In the *acceptor-side mechanism* [5], light-induced reduction of the plastoquinone pool promotes double reduction, protonation and loss of the $Q_A$ electron acceptor of PSII. When the $Q_A$ site is in one of these abnormal configurations, recombination reactions produce triplet chlorophyll (Chl) that may react with $O_2$ to produce harmful singlet oxygen. The *low-light hypothesis* [6] states that generation of triplet Chl in recombination reactions would explain photoinhibition when electron transfer is slow, i.e., under dim continuous light or under illumination by short flashes. The *donor-side mechanism* is based on the fact that the oxidized primary donor of PSII, $P_{680}^{+}$, has so high oxidative potential that it can oxidize pigment molecules if electron transfer from the oxygen-evolving complex (OEC) does not function. Donor-side photoinhibition has been directly observed after chemical inactivation of OEC [7–9], but it has also been hypothesized that this mechanism occurs in intact PSII because OEC sometimes fails to reduce $P_{680}^{+}$ [10]. We will call the latter

*Abbreviations:* Chl, chlorophyll; DLGA, DL-glyceraldehyde; DCBQ, 2,6-dichlorobenzoquinone; HEPES, 4-(2-hydroxyethyl)-1-piperazineethanesulfonic acid; PPFD, photosynthetic photon flux density; PFD, photon flux density; MV, methyl viologen; DCPIP, dichlorophenol-indophenol; DPC, diphenylcarbazide; PSII, photosystem II; UV, ultraviolet

* Corresponding author. Tel.: +358 2 3338078; fax: +358 2 3338075.
*E-mail address:* esatyy@utu.fi (E. Tyystjärvi).

0005-2728/$ - see front matter © 2004 Elsevier B.V. All rights reserved.
doi:10.1016/j.bbabio.2004.09.001

variant of the donor-side mechanism the *statistical donor-side mechanism*. The fourth main hypothesis, *singlet-oxygen hypothesis*, proposes that photoinhibition is caused by generation of singlet oxygen or other reactive oxygen species by iron–sulfur centers or cytochromes [11] or by uncoupled Chl [12]. In addition, light absorption by plastosemiquinone [13] or manganese [14] has been proposed to account for photoinhibition under UV or near-UV illumination.

Photoinhibition occurs both under anaerobic and aerobic conditions [2,5]. Because $Q_A$ double reduction and oxidative damage caused by $P_{680}^+$ are independent of oxygen, both acceptor- and donor-side mechanisms can function under anaerobic conditions. On the contrary, hypotheses explaining photoinhibition by the effects of singlet oxygen produced outside functional PSII do not explain the occurrence of photoinhibition under anaerobiosis. Thus, if singlet oxygen production outside PSII is the dominant mechanism of photoinhibition under aerobic conditions, a distinct pathway must function under anaerobic conditions. On the other hand, hypotheses based on production of singlet oxygen outside functional PSII are in agreement with the finding that the quantum yield of photoinhibition is the same under all light intensities [15,16], whereas acceptor-side photoinhibition occurs only under excess light, low-light photoinhibition under dim light, and donor-side photoinhibition is most pronounced under moderate light and is expected to saturate when the formation of long-lived $P_{680}^+$ saturates under bright light.

The finding that the rate of photoinhibition is directly proportional to light intensity from very low light to highly over-saturating light [16] suggests that, at least in part, photoinhibition proceeds through a mechanism that is independent of the rate of electron transfer through PSII. We studied further the relationship between photoinhibition and electron transport by varying light intensity and electron transport rate independently of each other, to identify their specific effects on photoinhibition. Our results revealed that indeed light intensity, not the rate of electron transfer nor the amount of excess energy, was the main factor determining the rate of photoinhibition. To get insight into this electron-transport-independent component, we compared the action spectrum of photoinhibition with the absorption spectra of different PSII components, such as aromatic amino acids, Chl, plastosemiquinone and manganese. The comparison indicated that the Mn cluster is apparently the photoreceptor of photoinhibition under UV light, and that the visible-light absorbance values of manganese compounds are so high that the manganese-related mechanism is important in visible light, too. We show that under both UV and visible light, photoinhibition proceeds largely with a mechanism that begins with inactivation of oxygen-evolving manganese complex, which predisposes PSII to damage caused by long-lived $P_{680}^+$.

## 2. Materials and methods

### 2.1. Plant material and isolation of thylakoids

Pea (*Pisum sativum* L.) and pumpkin (*Cucurbita pepo* L.) plants were grown under 150 μmol photons $m^{-2}$ $s^{-1}$ in a 12-h day/night rhythm. For in vivo experiments, thylakoids were isolated from control and treated leaves by grinding them in buffer containing 40 mM HEPES (pH 7.4), 0.3 M sorbitol, 10 mM $MgCl_2$, 1 mM ethylenediamine tetraacetic acid, 1 M glycine betaine and 1% bovine serum albumin. The suspension was centrifuged for 5 min at 1100×*g* and the pellet was suspended in osmotic shock buffer (10 mM HEPES (pH 7.4), 5 mM sorbitol and 10 mM $MgCl_2$). The centrifugation was repeated (2000×*g*) and the pellet was suspended in storage buffer (10 mM HEPES (pH 7.4), 0.5 M sorbitol, 10 mM $MgCl_2$ and 5 mM NaCl). In vitro experiments were done with pumpkin thylakoids isolated using the method described above and stored at −70 °C until use.

### 2.2. PSII activity measurements

Unless otherwise stated, the light-saturated rate of oxygen evolution was measured before and after photoinhibitory treatment with a Hansatech (King's Lynn, UK) oxygen electrode from isolated thylakoids (10 μg Chl $ml^{-1}$) by using 0.5 mM 2,6-dichlorobenzoquinone (DCBQ) as electron acceptor. The rate constant of photoinhibition ($k_{PI}$) was obtained by fitting the photoinhibitory loss of PSII activity to a first-order reaction equation and subtracting the rate constant of eventual dark inactivation. The quantum yield of photoinhibition was calculated by dividing $k_{PI}$ by the incident photosynthetic photon flux density (PPFD) and multiplying by the initial number of PSII centers in the sample, obtained by measuring the maximum flash-induced rate of oxygen evolution from a similar thylakoid preparation. Continuous 400–700-nm light was measured with a LI-185A quantum sensor (LICOR, Lincoln, NE).

### 2.3. Photoinhibition of DL-glyceraldehyde-treated leaves

The effect of Calvin–Benson cycle inhibitor, DL-glyceraldehyde (DLGA), on photoinhibition was studied using the second leaf pair of 2-week-old pea seedlings. The petioles were cut under water, placed in 2.3 mM lincomycin and kept under dim light (20 μmol photons $m^{-2}$ $s^{-1}$) for 1.5 h. DLGA was then added to 50 mM final concentration; water was added to control leaves. DLGA uptake through the petiole was allowed for 1 h under 100 μmol photons $m^{-2}$ $s^{-1}$. To induce photoinhibition, control and DLGA-treated leaves were illuminated with the petioles in the DLGA or control solutions at 600 or 1500 μmol photons $m^{-2}$ $s^{-1}$, as indicated, for 3.5 or 1.5 h, respectively. PSII activity was measured from thylakoids isolated from non-illuminated and illuminated leaves.

To verify that DLGA fully inhibited photosynthesis, oxygen evolution was measured from control and DLGA-treated leaves (both treated with lincomycin) with a Hansatech leaf disc oxygen electrode. These measurements were done without exposing the leaves to photoinhibitory illumination prior to measurement. The oxygen-evolution measurement was done at 20 °C under the PPFD of 1500 μmol $m^{-2}$ $s^{-1}$. $CO_2$ was provided by flushing the electrode cuvette with exhaled air. The effect of DLGA on the rate of electron transfer through PSII was measured with PAM-101 fluorometer (Heinz Walz GmbH, Effeltrich, Germany). Before the fluorescence measurement, control and DLGA-treated pea leaves were kept in darkness for 30 min. $F_0$ and $F_M$ were measured by illuminating the leaf with the measuring beam alone and with a 2-s saturating light pulse (PPFD 5500 μmol $m^{-2}$ $s^{-1}$), respectively. The leaf was then illuminated for 6 min at 600 or 1500 μmol $m^{-2}$ $s^{-1}$, as indicated, and a second saturating light pulse was fired to induce $F_M'$, followed by switch-off of all other light except for the measuring beam, to measure $F_0'$. The rate of absorption of excess photons (E) was calculated as $E=(F_M'-F_0')/F_M'\times(1-q_P)\times 0.5\times 0.84\times$PPFD, where $q_P$ is photochemical quenching and the factors 0.5 and 0.84 stand for the assumed PSII/(PSI+PSII) ratio and leaf absorptance, respectively [17].

### 2.4. Photoinhibition of isolated thylakoids treated with MV

Comparison of in vitro photoinhibition of thylakoids in the presence and absence of 120 μmol methyl viologen (MV) was done by illuminating 3 ml of thylakoid suspension (50 μg Chl $ml^{-1}$) in a 50-ml beaker at 20 °C with gentle stirring at 450 or 2300 μmol $m^{-2}$ $s^{-1}$, as indicated, for 60 or 10 min, respectively. Catalase (3000 U $ml^{-1}$) was added to all samples to protect the thylakoids from hydrogen peroxide. Preliminary experiments showed that the presence of superoxide dismutase (5 U $ml^{-1}$) in addition to catalase offered no extra protection in our thylakoid material (data not shown) and superoxide dismutase was therefore omitted. Ammonium chloride (5 mM) was added to both control and MV-treated samples to relieve the effect of photosynthetic control on electron transfer during photoinhibitory illumination.

The effect of MV on the reduction state of PSII electron acceptors in isolated thylakoids was measured with Chl fluorescence basically in the same way as in intact leaves. Thylakoids were dark adapted for 2 min, $F_0$ and $F_M$ were measured, and the 1.5-ml sample (10 μg Chl $ml^{-1}$) was then illuminated in a 1-cm spectrophotometer cuvette at 450 or 2300 μmol $m^{-2}$ $s^{-1}$, as indicated. After 7.5 min of actinic illumination, a 2-s saturating pulse was fired to induce $F_M'$, and then $F_0'$ was measured by switching off the actinic light. Absorptivity of the thylakoid sample between 400 and 700 nm was measured by integrating the product of the emission spectrum of the lamp and the transmission spectrum of thylakoid pigments in *N*,*N*-dimethylformamine; a similar absorptivity value was obtained by directly measuring the fraction of incident quanta transmitted through a 1-cm layer of intact thylakoids (data not shown). The rate of excess photon absorption was calculated as described by Demmig-Adams et al. [17], but replacing leaf area by the number of functional PSII centers per unit area of the thylakoid sample.

### 2.5. In vitro photoinhibition induced with short flashes and continuous light

Thylakoids (50 μg Chl $ml^{-1}$) were illuminated at 20 °C in 200-μl, 1-cm dia. stirred cuvettes sealed with Schott GG400 UV-blocking filters. Flash illumination (1 flash/4.7 s unless otherwise stated) was given with a FX-200 Xenon flash lamp (EG&G, Gaithersburg, MD) brought to 1-mm distance from the cuvette. The flash energy was varied with capacitors. At regular intervals, PSII activity was measured from one flashed and one non-flashed sample. The number of photons entering the cuvette through UV-blocking filter per one Xenon flash was measured by chemical actinometry at 475–610 nm [18]; the result was extended to the 400–700-nm range by comparison with the spectrum of the flash lamp. Continuous-light photoinhibition was induced with a slide projector lamp and the same cuvette setup was used as in flash illumination experiments.

Oxygen evolution under flash illumination was measured with a Hansatech oxygen electrode. A fused silica rod was used both as a light guide and a stopper [19]. The 310-μl thylakoid sample (100 μg Chl $ml^{-1}$) was illuminated with the FX-200 Xenon lamp through the fused silica rod at 10-Hz flash frequency. The number of photons entering the oxygen electrode chamber was measured actinometrically [18] in separate experiments. The maximum rate of oxygen evolution per four flashes was taken to represent the number of functional PSII centers in the thylakoid sample.

### 2.6. Action spectra of photoinhibition

Aerobic and anaerobic action spectra of photoinhibition were produced by illuminating thylakoids with an ozone-free continuous-light Xenon lamp (Model 6258, Oriel, Stratford, CT) through a water filter and pairs of LS and LL cutoff filters (Corion) defining 50-nm wavelength bands in visible region. The PPFD of the visible-light treatments was 200 μmol $m^{-2}$ $s^{-1}$. The 360- and 254-nm peaks (138 and 72 μmol photons $m^{-2}$ $s^{-1}$, respectively) were produced with an ENF-280C lamp (Spectronics, Westbury, NY). The number of UV photons entering our illumination cuvette was measured with ferrioxalate actinometry [20]. The $k_{PI}$ values were obtained from the loss of oxygen evolution, and the $k_{PI}$ values from the UV light treatments were corrected for differences in photon flux density according to the linear proportionality between $k_{PI}$ and light intensity [16]. Aerobic action spectrum of photoinhibition was done

by illuminating 5-ml thylakoid samples (50 μg Chl $ml^{-1}$; 2.4-mm light path). For illumination under anaerobic conditions, the photoinhibition buffer was bubbled with Argon, and 8 U/ml glucose oxidase, 6 mM glucose and 800 U/ml catalase were added to the 11-ml thylakoid sample (18 μg Chl $ml^{-1}$; 10-mm light path), and the cuvette was sealed gas-tightly. After the anaerobic photoinhibition treatment, the thylakoids were washed twice with the $O_2$ measurement medium before measuring $O_2$ evolution.

The action spectrum of photoinhibition of hydroxylamine-washed [7] thylakoids was produced by illuminating 800-μl thylakoid samples at 100 μmol photons $m^{-2}$ $s^{-1}$ of visible or UV light as described above. Before and after illumination, the light-saturated rate of reduction of 120 μM dichlorophenol-indophenol (DCPIP) in the presence of 2 mM diphenylcarbazide (DPC) was measured spectrophotometrically at 590 nm. A very slow endogenous rate of DCPIP reduction by DPC was subtracted, and $k_{PI}$ values were calculated from first-order fits of the loss of DCPIP reduction rate. Separate experiments with white light showed that the light response of photoinhibition of the hydroxylamine-washed thylakoids was directly proportional to photoinhibitory PPFD in the range of 50 to 150 μmol $m^{-2}$ $s^{-1}$ (data not shown).

Action spectrum of $O_2$ evolution was measured by illuminating thylakoids in an $O_2$ electrode through a fused silica rod, using the same filter combinations as described above. The light intensities were adjusted so that the rate of $O_2$ evolution was directly proportional to light intensity when the 400–450-nm filter pair was used.

### 2.7. OEC-dependent and independent PSII activities and Mn loss

For comparison of the kinetics of the loss of OEC-dependent and OEC-independent electron transfer activities of PSII and for Mn loss measurements, thylakoids were illuminated in the same way as in the action spectra measurements but using either 72 μmol photons $m^{-2}$ $s^{-1}$ of 254-nm UV-C light or 17 mmol photons $m^{-2}$ $s^{-1}$ of visible light, as indicated. A Schott GG-400 filter and an extra heat-absorbing glass blocked UV light in the visible-light experiments. The temperature of the visible light treatment was 20 °C and the UV-C treatments were done on ice. After illumination, OEC-independent PSII activity ($H_2O$+DPC to DCPIP) was measured as described above, and the OEC-dependent PSII activity ($H_2O$ to DCPIP) was measured similarly but in the absence of DPC. D1 protein was quantified immunologically after electrophoretic separation of thylakoid proteins as earlier described [21]. For measurements of lumen Mn content, non-illuminated and illuminated thylakoids were broken with a Yeda press at 100 bar. The suspension was then centrifuged at 300 000×$g$ for 30 min, and the Mn content of the supernatant was measured by plasma emission spectroscopy.

## 3. Results

### 3.1. Photoinhibition of DLGA-treated leaves

Photoinhibition damage in vivo is repaired via de novo synthesis of the D1 protein that is encoded by the chloroplast genome. To determine the actual rate of photoinhibition in vivo, we treated pea leaves with lincomycin, an inhibitor of chloroplast protein synthesis. Photoinhibition of lincomycin-treated pea leaves was compared in the presence and absence of DLGA, a specific inhibitor of the Calvin–Benson cycle [22]. The leaves were illuminated under the PPFD of 600 or 1500 μmol $m^{-2}$ $s^{-1}$, as indicated. Thylakoids were isolated from non-illuminated and illuminated leaves and light-saturated oxygen evolution was measured from these thylakoids in the presence of the artificial electron acceptor DCBQ. The first order rate constant of photoinhibition ($k_{PI}$; see Ref. [16]) was calculated from the decrease in the oxygen evolution rate during illumination. The results showed that photoinhibition proceeded slightly more slowly in DLGA-treated than in control leaves at both 600 and 1500 μmol photons $m^{-2}$ $s^{-1}$ (Fig. 1A).

To confirm that the DLGA treatment actually inhibited photosynthesis, we measured oxygen evolution from leaf discs under the PPFD of 1500 μmol $m^{-2}$ $s^{-1}$ and found that the DLGA-treated leaves did not evolve any oxygen (Table 1). Furthermore, fluorescence quenching analysis showed that the electron acceptor $Q_A$ was fully reduced and the electron transfer rate was almost zero in the DLGA-treated leaves during illumination (Fig. 1B and Table 2). DLGA had no direct inhibitory effect on PSII, as the in vitro rate of oxygen evolution in the presence of artificial electron acceptor, DCBQ, measured before the photoinhibitory treatment, was similar in thylakoids isolated from the lincomycin treated leaves and from the leaves treated with lincomycin and DLGA (Table 1). In earlier experiments by Hollinderbäumer et al. [23], DLGA treatment was shown to enhance photoinhibition, but in their experiments concurrent repair of PSII was not prevented during illumination, and thus the enhancing effect of DLGA on loss of PSII activity was probably due to decrease in D1 synthesis, which apparently requires functional photosynthesis.

The rate of photoinhibition and excess energy generally show a positive correlation, because both excess energy and the rate constant of photoinhibition are directly proportional to light intensity. The fluorescence quenching data allowed us to calculate the number of excess photons absorbed by the leaf but neither used for photochemistry nor dissipated by the light-inducible excitation quenching mechanisms [17]. DLGA treatment doubled the amount of excess photons under 600 μmol photons $m^{-2}$ $s^{-1}$ and greatly increased excess energy also at 1500 μmol photons $m^{-2}$ $s^{-1}$ (Table 2). When excess energy and photoinhibitory efficiency were compared in control and DLGA-treated leaves

at the same light intensity (Fig. 1C, dashed lines), the relationship showed negative correlation: the more excess energy, the less photoinhibition.

### 3.2. Effect of MV on photoinhibition of isolated thylakoids

The DLGA treatment led to decrease in photochemical quenching. To test the effect of an increase in photochemical quenching under unchanged light intensity, we photoinhibited isolated thylakoids in the absence and presence of MV, a potent electron acceptor of PSI. Catalase was added to prevent nonspecific damage caused by the oxygen radicals and hydrogen peroxide arising due to the autooxidation of MV. Photoinhibition proceeded slightly faster in the presence than in the absence of MV at both 450 and 2300 μmol photons $m^{-2}$ $s^{-1}$ (Fig. 2A). Fluorescence quenching analysis showed that the electron acceptor MV increased the electron transfer rate and thereby significantly lowered the excitation pressure of PSII, especially at the lower PPFD of 450 μmol $m^{-2}$ $s^{-1}$ (Fig. 2B and Table 2), and that MV treatment efficiently decreased the amount of excess energy under both 450 and 2300 μmol photons $m^{-2}$ $s^{-1}$ (Table 2). Again, a slightly negative correlation was obtained between $k_{PI}$ and excess energy when samples illuminated in the presence and absence of MV were compared at the same light intensity (Fig. 2C, dashed lines).

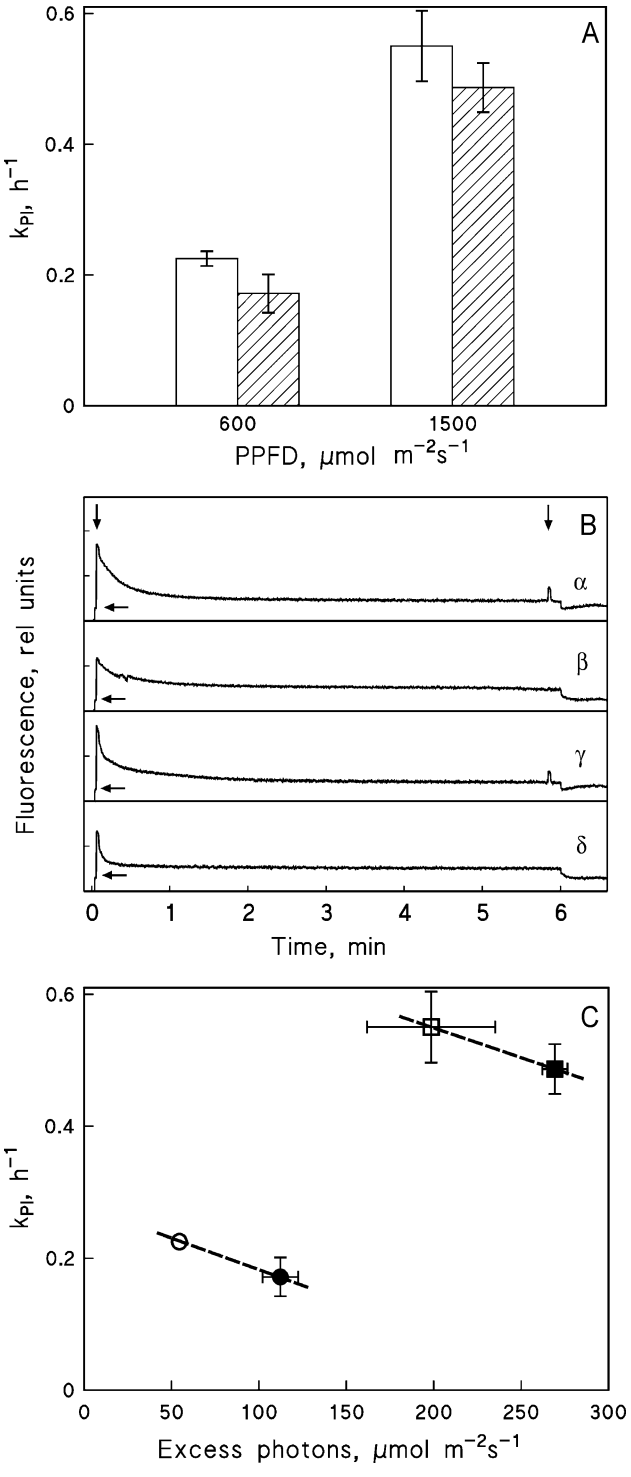


Fig. 1. Effect of DLGA on photoinhibition. (A) The in vivo rate constant of photoinhibition, measured from lincomycin-treated pea leaves illuminated in the absence (open bars) and presence (hatched bars) of 50 mM DLGA. Photoinhibition was induced by illuminating leaves for 3.5 h at the PPFD of 600 μmol $m^{-2}$ $s^{-1}$ or for 1.5 h at 1500 μmol $m^{-2}$ $s^{-1}$, as indicated, and the $k_{PI}$ values were obtained by comparing the oxygen-evolution activity ($H_2O$ to DCBQ) of thylakoids isolated from illuminated leaves to thylakoids isolated from non-illuminated leaves. (B) Fluorescence measurements from non-photoinhibited lincomycin treated pea leaves in the absence (traces α and γ) and presence of 50 mM DLGA (traces β and δ). After dark adaptation, the $F_0$ value was measured (horizontal arrow) and then the leaves were illuminated at the PPFD of 600 μmol $m^{-2}$ $s^{-1}$ (traces α and β) or 1500 μmol $m^{-2}$ $s^{-1}$ (traces γ and δ). Two saturating flashes were applied as indicated by the vertical arrows. (C) $k_{PI}$ of control leaves (open symbols) and of DLGA-treated leaves (solid symbols) (data from A) as a function of the number of excess photons (data from Table 2). The dashed line connects photoinhibition experiments at the PPFD of 600 μmol $m^{-2}$ $s^{-1}$ (circles) and those done at 1500 μmol $m^{-2}$ $s^{-1}$ (squares). In A and C, error bars, drawn if larger than the respective symbol, show S.D. ($n$=3).

Table 1
In vivo and in vitro oxygen evolution rates of non-illuminated samples

| Sample | Oxygen evolution in leaves ($H_2O$ to $CO_2$), μmol $O_2$ $cm^{-2}$ $h^{-1}$ | Oxygen evolution in thylakoids ($H_2O$ to DCBQ), μmol $O_2$ mg $Chl^{-1}$ $h^{-1}$ |
|---|---|---|
| Control leaves | 6.8±0.3 | 163±4 |
| DLGA leaves | 0 | 156±3 |
| Control thylakoids | | 245±3 |
| MV thylakoids | | 239±4 |

In vivo oxygen evolution rates were measured with a leaf disc oxygen electrode at saturating $CO_2$ concentration under the PPFD of 1500 μmol $m^{-2}$ $s^{-1}$ from control and DLGA-treated leaves, both treated with lincomycin. The in vitro oxygen evolution rates were measured in the presence of an exogenous electron acceptor either from thylakoids isolated from control and DLGA-treated pea leaves (both treated with lincomycin) or from non-treated pumpkin thylakoids in the presence of catalase or in the presence of MV and catalase. Oxygen evolution in thylakoids was measured at saturating PPFD with a suspension-type oxygen electrode, using DCBQ as electron acceptor. The values represent the mean and S.D. of at least three independent experiments.

Table 2
Photochemical quenching, electron transport rate and the number of excess photons measured from control and DLGA-treated pea leaves and from control and MV-treated thylakoid samples

| Sample | PPFD, μmol $m^{-2}$ $s^{-1}$ | Photochemical quenching ($q_P$) | Electron transfer rate | Excess photons |
|---|---|---|---|---|
| Control leaves | 600 | 0.66±0.03 | 107±6.8 | 54±4.4 |
| | 1500 | 0.45±0.11 | 165±47 | 199±37 |
| DLGA leaves | 600 | 0.03±0.05 | 1.7±3.4 | 112±10 |
| | 1500 | 0±0 | 0±0 | 269±7.1 |
| Control thylakoids | 450 | 0.22±0.11 | 34±3.4 | 306±13 |
| | 2300 | 0.01±0.00 | 17±4.1 | 1380±19 |
| MV thylakoids | 450 | 0.47±0.02 | 132±1.5 | 149±13 |
| | 2300 | 0.14±0.02 | 161±15 | 1010±79 |

Both control and DLGA leaves were treated with lincomycin, and catalase was present in both control and MV-treated thylakoids samples. The values were calculated from fluorescence measurements like those shown in Figs 1B and 2B, and each value represents the mean and S.D. of at least three independent experiments. When calculating the electron transport rate and the number of excess photons, the PSII:PSI stoichiometry was assumed to be 1:1 and the leaves were assumed to absorb 84% of incident quanta; the thylakoid samples were measured to absorb 56%. The electron transfer rates and excess photons are expressed as μmol $m^{-2}$ $s^{-1}$ for leaves and $PSII^{-1}$ $s^{-1}$ for thylakoids.

### 3.3. In vitro photoinhibition induced with short flashes and continuous light

Photoinhibition experiments in the presence of DLGA or MV showed that the rate of electron transfer had only a minor influence on the rate of photoinhibition (Figs. 1A and 2A). To further study the relationship between photoinhibition and electron transfer rate, we used short flashes of light to measure the ratio between $k_{PI}$ and PPFD. For the measurement of flash-induced photoinhibition, thylakoids were enclosed in a small cuvette under a UV-blocking filter, and illuminated with 5-μs Xenon flashes. The flashes were fired at 4.7-s intervals, unless otherwise stated. The single turnover Xenon flashes were supersaturating with regard to oxygen evolution (Fig. 3A), thus inducing one electron transfer event ($S_nQ_A \rightarrow S_{n+1}Q_A^-$; $S_n$ denoting the $n$th S-state of OEC) per flash per PSII, followed by a moderate number of back reactions ($S_nQ_B^- \rightarrow S_{n-1}Q_B$), irrespective of the flash intensity. The background was dim laboratory light of 1–2 μmol photons $m^{-2}$ $s^{-1}$. Oxygen evolution activity was measured from the thylakoid samples before and after the photoinhibitory illumination. The results show that photoinhibition proceeded more rapidly when the intensity of the supersaturating flashes was increased (Fig. 3B), and the $k_{PI}$ values were directly proportional to the flash intensity (Fig.

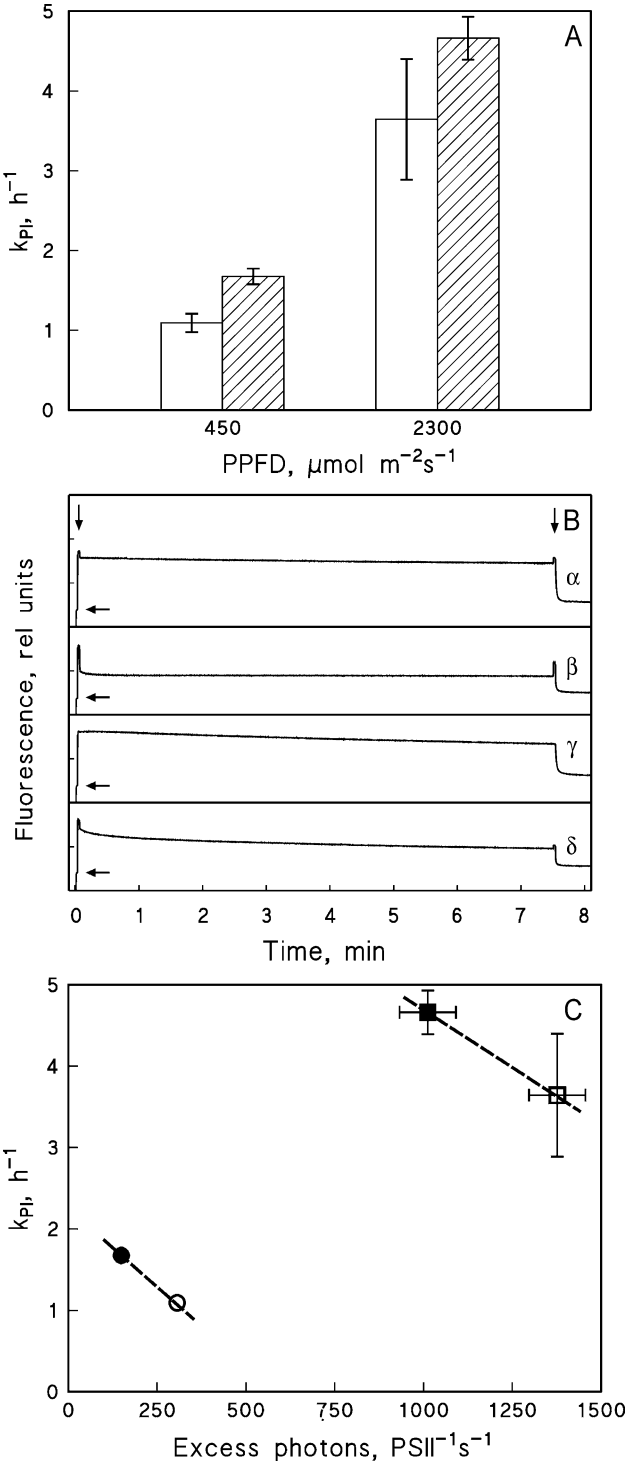


Fig. 2. Effect of MV on photoinhibition. (A) The in vitro rate constant of photoinhibition, measured from isolated pumpkin thylakoids illuminated in the absence (open bars) or presence (hatched bars) of 120 μM MV. Catalase was present in all samples. Photoinhibition was induced by illuminating the thylakoid samples for 60 min at the PPFD of 450 μmol $m^{-2}$ $s^{-1}$ or for 10 min at the PPFD of 2300 μmol $m^{-2}$ $s^{-1}$, as indicated, and the $k_{PI}$ values were obtained by comparing the oxygen-evolution activity ($H_2O$ to DCBQ) before and after the photoinhibitory illumination. (B) Fluorescence measurements from non-photoinhibited thylakoids in the absence (traces α and γ) and in the presence of MV (traces β and δ). After dark adaptation, the $F_0$ value was measured (horizontal arrows) and then the thylakoids were illuminated at the PPFD of 450 (traces α and β) or 2300 (traces γ and δ) μmol $m^{-2}$ $s^{-1}$. Two saturating flashes were applied as indicated by the vertical arrows. (C) $k_{PI}$ of thylakoids photoinhibited in the absence (open symbols) or presence (solid symbols) of MV (data from A) as a function of the number of excess photons (data from Table 2). The dashed line connects photoinhibition experiments done at the PPFD of 450 μmol $m^{-2}$ $s^{-1}$ (circles) and those done at 2300 μmol $m^{-2}$ $s^{-1}$ (squares). In A and C, error bars, drawn if larger than the respective symbol, show S.D. ($n$=3).

3C, circles). The average PPFD values of the flash photoinhibition treatments were calculated by measuring the number of photons delivered by each flash to the cuvette, and by multiplying the result by the flashing frequency. Flash-light-induced photoinhibition was then compared with continuous-light-induced photoinhibition using the same cuvette system. The ratio between $k_{PI}$ and PPFD remained the same under continuous light (Fig 3C, squares) as under illumination with 5-μs Xenon flashes. The quantum yield of photoinhibition, calculated from the data in Fig. 3C, is approximately $2\times10^{-7}$ and the similarity of the quantum yield of photoinhibition under continuous and flash illumination supports the conclusion that continuous-light-induced photoinhibition contains a significant component which is independent of PSII electron transport.

According to the low-light photoinhibition mechanism [6], the flashing rate has a major influence on the rate of photoinhibition. To test if our flash-induced photoinhibition obeyed the predictions of the low-light mechanism, we induced photoinhibition with multiple flashing rates. In our experiments, changing the flash-to-flash delay from 4.7 to 18.8 s (Fig. 3C, diamond), doing the flash treatment in full darkness (Fig. 3C, solid circles) or using flash pairs with 1 s between the flashes of the pair and 9.6 s between the pairs (Fig. 3C, triangle) did not affect the ratio between $k_{PI}$ and average PPFD. Furthermore, flashes fired at flash-to-flash delay of 1 s had the same photoinhibitory efficiency as flashes fired at the flash-to-flash delay of 4.7 s (data not shown). These results indicate that Xenon flashes caused photoinhibition in the same way as continuous light rather than with the low-light mechanism.

### 3.4. Action spectra of anaerobic and aerobic photoinhibition

Next, we tested if production of singlet oxygen outside PSII can account for the electron-transport-independent component of photoinhibition. Singlet oxygen can only be generated in the presence of oxygen, and therefore photosensitizers producing singlet oxygen would be recognized by comparing the action spectrum of photoinhibition under anaerobic and aerobic conditions. This comparison showed

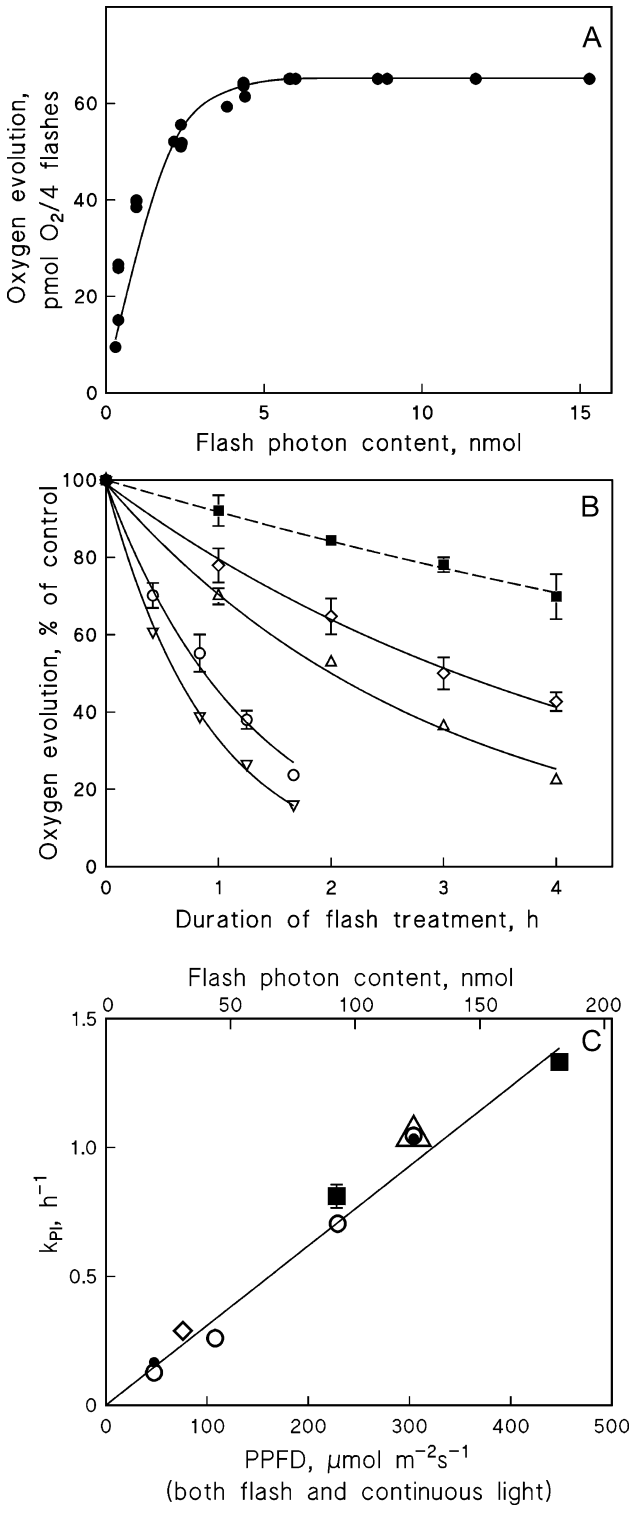


Fig. 3. Flash-light-induced photoinhibition. (A) The light response curve of oxygen evolution obtained by illuminating thylakoids (35 μg Chl) with 5-μs flashes from a Xenon flash lamp at the frequency of 10 flashes/s. Oxygen evolution was measured with a Hansatech oxygen electrode, using a quartz bar both as a stopper and a light guide. Each symbol represents one determination of the oxygen evolution rate. The flash energy range is 0 to 2 J/flash. (B) Time course of photoinhibition of oxygen evolution activity during illumination of thylakoids with Xenon flashes fired at the rate of 1 flash/4.7 s. The flash energies were 1.3 J (diamonds), 3.7 J (upward triangles), 11.4 J (circles) and 14.6 J (downward triangles). Loss of PSII activity in the absence of flash illumination is also shown (solid squares). The lines show the best fit to a first-order reaction equation. Each data point represents the mean of three to four independent experiments. (C) $k_{PI}$ measured under Xenon flash illumination (circles, diamond, triangle) and under continuous light (squares), as a function of PPFD. The $k_{PI}$ values have been corrected by subtracting the rate constant of dark inactivation. Thylakoids were illuminated in 200-μL cuvettes, protected with an UV absorbing filter. The delay between the flashes was 4.7 s (circles) or 18.8 s (diamond); flash pairs with 1 s between the flashes of the pair and 9.4 s between the pairs were also tested (triangle). The flash treatments were done under dim laboratory light, PPFD 1–2 μmol $m^{-2}$ $s^{-1}$ (open symbols; data from B), or in darkness (solid circles). In B and C, error bars, drawn if larger than the respective symbol, show S.E. ($n$=3).

that the action spectra of aerobic and anaerobic photoinhibition are essentially similar and no peaks, specific to aerobic conditions, can be seen (Fig. 4A). This result strongly suggests that the contribution of singlet oxygen produced outside PSII was small in our thylakoid material, which limits the possible photoreceptors to constituents of PSII.

### 3.5. Oxygen evolving manganese complex is the target of UV-induced photoinhibition

The photoinhibitory efficiency of light in intact thylakoids is high in UV-C and decreases steadily towards the visible range, staying low and relatively constant above 450 nm (Fig. 4B and C). In order to localize the photoreceptor, we measured the action spectrum of photoinhibition from thylakoids that had been pretreated with hydroxylamine to wash off the oxygen evolving manganese complex. Fig. 4B shows that the removal of OEC changed the action spectrum of photoinhibition radically, revealing that the reaction center of OEC-less PSII is remarkably resistant against UV light. Furthermore, an apparent similarity between the action spectrum of photoinhibition in OEC-less thylakoids and the action spectrum of PSII oxygen evolution was revealed (Fig. 4B) suggesting that if OEC is damaged, then photodamage to the PSII reaction center occurs due to light absorption by Chl. This is in accordance with earlier data showing that photodamage to Mn-less thylakoids is caused by the primary donor of PSII [7–9].

The similarity of aerobic and anaerobic photoinhibition (Fig. 4A) limits the search for the main photoreceptors of photoinhibition to constituents of PSII, and Fig. 4B shows that the compound responsible for the UV-sensitivity of PSII is part of the OEC and washes off with hydroxylamine. These data exclude plastosemiquinone (Fig. 4D) and the tyrosine (Fig. 4D) residues of D1 protein as photoreceptors of photoinhibition, because these UV-absorbing compounds are not washed off with hydroxylamine. From the proteins and metal cofactors of the OEC, only manganese ions and tyrosine and tryptophan (Fig. 4D) residues of the 33-, 23- and 16-kDa proteins show absorption in the 220- to 400-nm range. However, the extinction coefficients of the aromatic amino acids decrease sharply before or at 300 nm (Fig. 4D), indicating that the UV absorption by these compounds does not significantly contribute to photoinhibition. In addition to

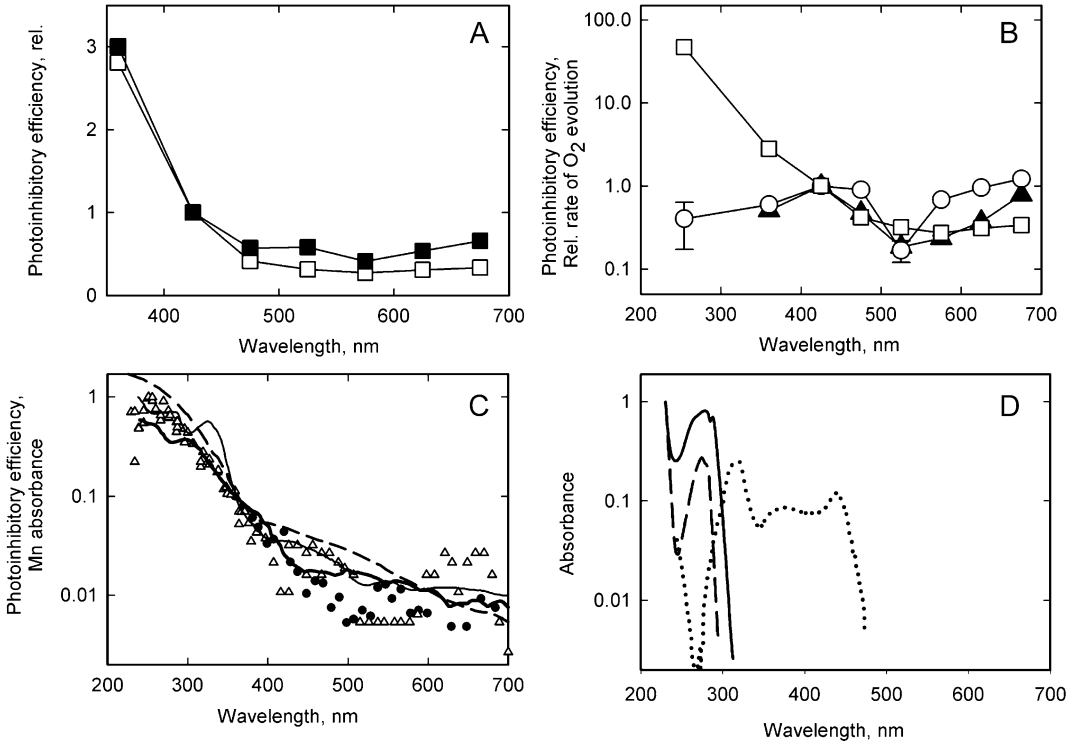


Fig. 4. Action spectra of photoinhibition. (A) Action spectrum of photoinhibition of isolated thylakoids illuminated under aerobic (open squares) or anaerobic conditions (solid squares). The spectra are normalized to the value at 400–450 nm to facilitate comparison in the visible range. (B) Action spectrum of the loss of electron transfer from DPC to DCPIP in OEC-less thylakoids (donor-side photoinhibition) (circles) in comparison with the action spectrum of photoinhibition in intact thylakoids (squares). Triangles show the action spectrum of oxygen evolution in intact thylakoids. The spectra are normalized to the value at 400–450 nm, and a logarithmic ordinate axis is used. Error bars, drawn if larger than the respective symbol, show SE ($n$=3). (C) Action spectra of photoinhibition published by Jones and Kok [15] (open triangles) and by Jung and Kim [11] (solid circles) in comparison with the absorption spectra of three manganese model compounds: 5 mM Mn(III)gluconate in 0.01 M gluconate (Ref. [26]; dashed line), Mn(III)-*O*-Mn(IV)-(*N*,*N*-bis(2-pyridylmethyl)-*N*′-salicyliden-1,2-diaminoethane)$_2$ (Ref. [28]; thick solid line) and [$Mn_2$(III,IV)(μ-O)$_2$(2,2′:6,2″-terpyridine)$_2$($CF_3CO_2$)$_2$]$^+$ (Ref. [29]; thin solid line). The spectra are normalised so that the value at 360 nm is 0.1, and a logarithmic ordinate axis is used to facilitate comparison of the whole range. (D) Absorption spectra of tyrosine (dashed line), tryptophan (solid line) and plastosemiquinone (dotted line). These spectra are redrawn from Ref. [46].

the Chl antenna of PSII (see action spectrum in Fig. 4B), also manganese compounds absorb throughout the visible range (Fig. 4C). Thus, further discussion about the photoreceptors of photoinhibition can be limited to the manganese ions of OEC and to the Chl antenna of PSII.

The comparison of the action spectrum of photoinhibition with the absorption spectra of Mn(III) and Mn(IV) ions, which are found in functional OEC during the oxygen evolving S-state cycle [24,25], revealed remarkable similarity throughout the whole UV and visible wavelength range (Fig. 4C). We used the absorption spectra of three different OEC-model Mn compounds in comparison; manganese(III)gluconate [26], which has been used as the spectral basis of difference spectroscopy of the S-states [27], and two OEC model compounds containing oxo-bridged Mn(III) and Mn(IV); Mn(III)-*O*-Mn(IV)-(*N*,*N*-bis(2-pyridylmethyl)-*N*′-salicyliden-1,2-diaminoethane)$_2$ [28] and [$Mn_2$(III,IV)(μ-O)$_2$(2,2′:6,2″-terpyridine)$_2$($CF_3CO_2$)$_2$]$^+$ [29]. The similarity between the action spectrum of photoinhibition and the absorption spectra of the manganese model compounds is obvious in the UV range (Fig. 4C), indicating that manganese is the photoreceptor of photoinhibition in UV light. In the visible-light range, the absorption spectra of the manganese model compounds differ from each other. However, absorbance values of Mn complexes in visible wavelengths and the photoinhibitory efficiency of visible light are both at the same overall level compared to their corresponding values under UV light (Fig. 4C). Therefore, assigning Mn as the photoreceptor of photoinhibition in UV light implies that absorption of light by Mn will inevitably cause some photoinhibition in the visible range, too.

### 3.6. Oxygen evolution is lost in photoinhibition before damage to electron transfer chain

Photodamage of the oxygen-evolving manganese complex represents an electron-transfer-independent mechanism of photoinhibition. If this mechanism contributes significantly to photoinhibition, then the photoinhibitory loss of OEC activity would precede the eventual inhibition of other parts of the PSII electron transfer chain. We studied the order of inhibition of the OEC and the PSII reaction center by comparing the rate of PSII electron transport in the presence and absence of an exogenous electron donor DPC that mediates PSII electron transport even if OEC does not function. DCPIP was used as an electron acceptor. These measurements showed that under UV light, inhibition of OEC-dependent electron transfer from $H_2O$ to DCPIP preceded inhibition of OEC-independent electron transfer from DPC and $H_2O$ to DCPIP (Fig. 5A), confirming that OEC is the primary target of UV-induced photoinhibition. Fig. 5B shows that the precedence of the inhibition of OEC persisted under strong visible light, but the delay between inhibition of OEC-dependent and OEC-independent electron transport was much shorter than under UV light.

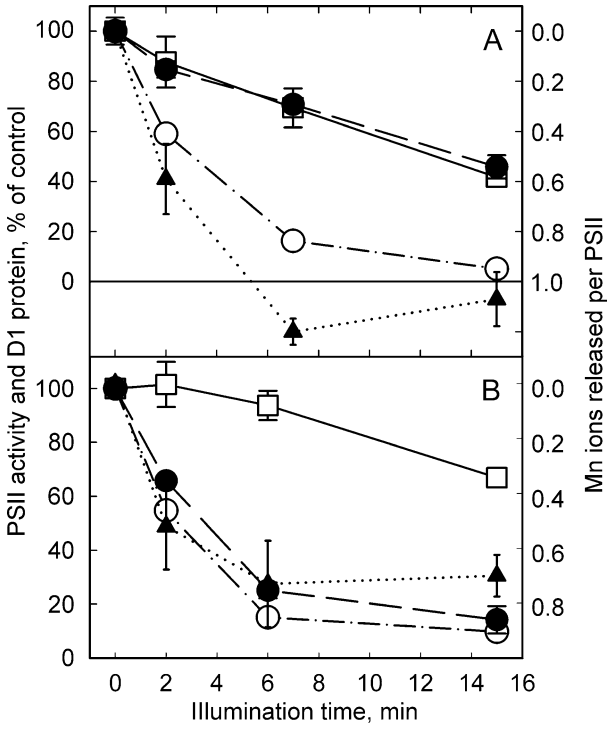


Fig. 5. Photoinhibition and release of manganese to thylakoid lumen during (A) UV light treatment (254 nm; 72 μmol photons $m^{-2}$ $s^{-1}$) or (B) strong visible light treatment (17 mmol $m^{-2}$ $s^{-1}$). Loss of OEC-dependent PSII electron transfer activity ($H_2O$ to DCPIP; open circles); loss of OEC-independent PSII activity (DPC+$H_2O$ to DCPIP; solid circles); release of Mn to the lumen (triangles) and loss of the D1 protein (squares). Error bars, drawn if larger than the respective symbol, show SE ($n$=3). Error bars belonging to Mn release have a short dash at top and bottom; other error bars have long dashes.

### 3.7. Manganese release is an early step in photoinhibition

We measured the Mn content of the thylakoid lumen before and after short photoinhibition treatments with UV or intense visible light. The lumen of control thylakoids contained approximately 0.5 Mn ions per PSII. Both under UV (Fig. 5A) and visible light (Fig. 5B), the Mn content of lumen increased by one Mn per one PSII center that had lost OEC activity, and this similarity in the stoichiometry was particularly obvious at the very early time points of the photoinhibition treatment. The kinetics of Mn release was notably faster than the kinetics of the decrease in the D1 protein content of the thylakoids (Fig. 5), indicating that secondary release of manganese due to D1 degradation [30] does not explain Mn release during the early phases of photoinhibition.

## 4. Discussion

### 4.1. Relationship between photoinhibition and excess energy

The mechanisms of photoinhibition of PSII have been under debate for several decades [31]. Because photo-

inhibition was first seen only if plants were exposed to high light intensities, it was initially assumed that the damage is caused by excess excitation energy. Excess energy has later been defined as energy that is absorbed by PSII but is neither used in photochemistry nor safely dissipated by light-inducible non-photochemical quenching [17]. From the viewpoint of the mechanisms of photoinhibition, excess energy is a complicated concept because the definition of excess energy assumes that photochemical and non-photochemical quenching have the same effect. Non-photochemical quenching has been shown to have no effect or a slight protective effect on photoinhibition [32,33] whereas conditions that lead to increase in excess energy by decreasing photochemical quenching actually protect against photoinhibition (Figs. 1C and 2C). Contrary to our result, slightly positive correlations between excess energy and the rate constant of photoinhibition were obtained when nitrogen fertilization or different growth light conditions were used to modulate excess energy [34,35], apparently because these treatments affect both photochemical and non-photochemical quenching. Altogether, both non-photochemical and photochemical quenching have only a minor effect on the rate of photoinhibition, which suggests that a significant part of photoinhibition is not caused by PSII electron transfer events after absorption of light by PSII antenna. This conclusion is supported by the finding that the quantum yield of photoinhibition is similar under continuous light and under illumination with single-turnover flashes fired at 1–18.8 s intervals (Fig. 3C), although flash illumination induces remarkably fewer electron transfer events per unit time than continuous light.

In donor-side photoinhibition, the photon that causes the formation of the damaging species, $P_{680}^{+}$, is by definition photochemically quenched. Thus, photochemical quenching enhances $P_{680}^{+}$-induced damage, although photochemical quenching lowers excess energy. Slight enhancement of photoinhibition by increased photochemical quenching occurred in our experiments (Figs. 1 and 2), suggesting that $P_{680}^{+}$-related damage has a role in photoinhibition both in vivo and in vitro. This enhancing effect of photochemical quenching on $P_{680}^{+}$-induced photoinhibition has been earlier seen in OEC-less PSII reaction centers in which photoinhibition occurs rapidly only if an electron acceptor ensures efficient oxidation of reduced $Q_A$ [36].

The finding that $P_{680}^{+}$ plays a role in photoinhibition might suggest that the statistical donor-side mechanism is a major component in photoinhibition. However, statistical donor-side mechanism is not in accordance with other features of photoinhibition. First, statistical donor-side photoinhibition is expected to have a similar action spectrum as was measured from OEC-less thylakoids but the action spectrum of photoinhibition in OEC-less thylakoids is notably different from the action spectrum of photoinhibition measured from intact thylakoids (Fig. 4C). Second, the formation of long-lived $P_{680}^{+}$ would become saturated under intense light, but light saturation of photoinhibition of intact PSII has never been reported, and the present data show that the ratio between the rate constant of photoinhibition and light intensity remains constant even under extremely high momentary irradiance (Fig. 3C). These data suggest that statistical donor-side photoinhibition does not have a dominating contribution to photoinhibition in general.

The acceptor-side mechanism requires intense light to reduce the plastoquinone pool [5], and therefore acceptor-side photoinhibition cannot explain why photons of low continuous light or short flashes cause photoinhibition with the same quantum efficiency as photons of intense continuous light (Fig. 3; Ref. [16]). The acceptor-side mechanism also predicts that the rate of photoinhibition always increases with PSII excitation pressure, but our results (Figs. 1 and 2), as well as earlier data [37,38], indicate that increase in the excitation pressure of PSII as such does not enhance photoinhibition. These data suggest that the contribution of the acceptor-side pathway to PSII photoinhibition is minor both in vivo and in vitro. The main evidence for the acceptor-side mechanism is that this mechanism predicts that photoinhibited PSII produces singlet oxygen, which has indeed been detected [39,40]. However, it is possible that only a small number of PSII become inhibited via the acceptor-side mechanism, and these ones produce the detected singlet oxygen. An alternative explanation for the production of singlet oxygen by photoinhibited leaves is that singlet oxygen originates from the light-harvesting complex II that may have lost the connection to the reaction center during the PSII repair [2]. Disconnected light-harvesting complex II has been shown to produce singlet oxygen in vitro [41].

Significant photoinhibition caused by singlet oxygen sensitizers outside of functional PSII [11,12] could not be verified in the present study. First, the absence of oxygen did not protect our thylakoid preparations against photoinhibition, and second, the aerobic action spectrum of photoinhibition did not contain any significant peaks missing from the anaerobic spectrum (Fig. 4A). Thus, our data support the conception that photoinhibition originates in functional constituents of PSII and that anaerobic and aerobic photoinhibition have essentially the same mechanism.

### *4.2. Electron-transport-independent photoinhibition is the visible-light tail of the UV mechanism*

Our data strongly support the hypothesis that the oxygen-evolving manganese complex is the target and photoreceptor of UV-induced photoinhibition. First, Mn-less PSII is stable under UV light (Fig. 4B; Ref. [14]) and the action spectrum of photoinhibition is similar to the absorption spectra of Mn(III) and Mn(IV) compounds in the UV range (Fig. 4C). Second, oxygen evolution activity is lost during UV-induced photoinhibition before the loss of electron transfer activity from $P_{680}$ to $Q_A$ (Fig. 5A). Furthermore, the

stoichiometric loss of one Mn per PSII during the early phase of UV-induced photoinhibition (Fig. 5A) suggests that the primary reaction in UV-induced photoinhibition is the release of a Mn ion from OEC to the thylakoid lumen. The finding that different S-states are differently susceptible to UV-induced photoinhibition [42] provides further evidence for the key role of Mn in UV-induced photoinhibition.

Because the data strongly suggest that the oxygen-evolving manganese complex is the photoreceptor of photoinhibition in UV light, we have to consider the consequences for the visible light range, too. The absorption spectra of different Mn(III) and Mn(IV) compounds vary considerably in the visible range (Fig. 4C; see also Refs. [26,28,29]), but the fact that all relevant Mn compounds show significant absorbance in the visible region implies that Mn contributes to photoinhibition in visible light. Our experiments demonstrate that the same Mn-related feature is present in photoinhibition under visible light as under UV light: the release of Mn to lumen and inhibition of OEC occur before the inhibition of electron transfer from $P_{680}$ to $Q_A$. Mn loss from damaged PSII has been reported earlier, but Mn release was interpreted to be a late event, possibly related to D1 protein degradation, rather than the primary cause of photoinhibition [30,43]. However, our data show that loss of manganese occurs early in photoinhibition under both visible (Fig. 5B) and UV light (Fig. 5A). Under visible light, the damage to OEC only slightly precedes the damage to the rest of PSII, because when OEC is damaged, the oxidizing $P_{680}^+$ damages the reaction center more rapidly under visible light than under UV light. Under strong visible light we were able to separate these two concurrent damaging reactions because strong light partially saturates electron transfer from $P_{680}$ to $Q_A$ and the consequent damage caused by $P_{680}^+$, but the rate of Mn-targeted inactivation of OEC is not light-saturated.

The role of the oxygen-evolving Mn complex in photoinhibition is further supported by the action spectrum of photoinhibition in the cyanobacterium *Synechocystis* sp. PCC 6803 in which blue-violet light (400–450 nm) has greater photoinhibitory efficiency than orange light (600–650 nm) although orange light is more efficiently absorbed by the phycobilisome antenna of cyanobacterial PSII [44]. In addition, action spectrum measurements around the red peak of Chl absorption suggest that PSII antenna may not be the main photoreceptor of photoinhibition even in red light in plant thylakoids [12].

The quantum yield of manganese excitation deserves attention because it constitutes an upper limit for the quantum yield of photoinhibition. The ratios of the extinction coefficients of the Chls to those of Mn(III) and Mn(IV) compounds [26–29] are between 100 and 1000 in visible light, depending on wavelength, and thylakoids contain one functional Mn per approximately 100 Chls. Thus, although Mn compounds show low absorbance in the visible range, the Mn ions of OEC would absorb one incident photon out of $10^4$–$10^5$. This number is 10–100 times bigger than the quantum yield of photoinhibition (Fig. 3; Ref. [16]), indicating that Mn-based reactions may contribute to photoinhibition under visible light. Light-induced breakage of the coordination bonds that hold the Mn ions in OEC may occur because excitation (d–d′ transition) changes the electronic configuration of Mn. A synthetic model compound of the functional Mn cluster [45] decomposes under 488-nm laser illumination (G. Brudvig, personal communication), suggesting that light-induced ligand loss occurs in Mn complexes.

The main mechanisms of photoinhibition are described in Fig. 6. The manganese-dependent mechanism (Fig. 6A) is the only one that can explain a major part of photoinhibition occurring under different conditions. The damage begins

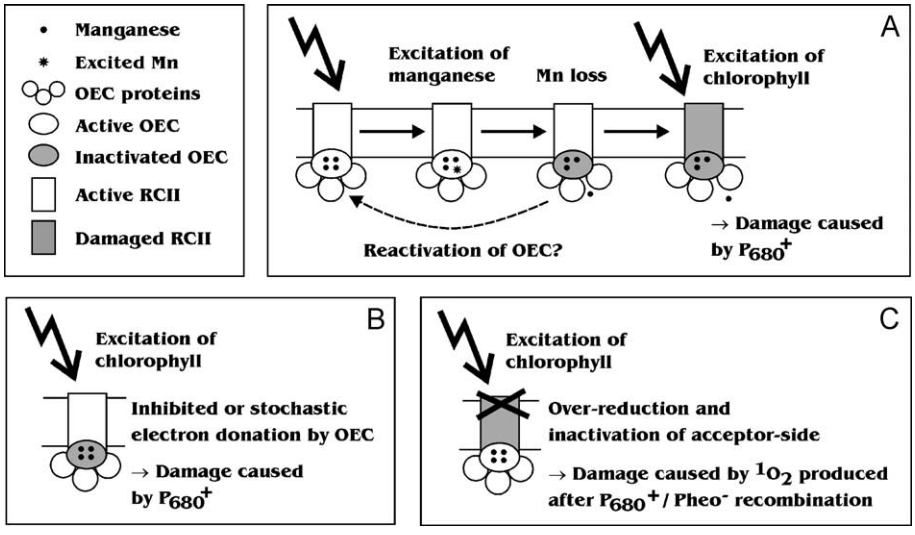


Fig. 6. Main mechanisms of photoinhibition. (A) Manganese-dependent photoinhibition, (B) statistical donor-side photoinhibition and (C) acceptor-side photoinhibition.

with excitation of a Mn ion of the OEC. The excited Mn leaves its site, which renders OEC incapable of donating an electron to $P_{680}^{+}$, which may then damage the PSII reaction center. We do not know if rebinding of Mn can occur after the light-induced inactivation. This mechanism is in agreement with the action spectrum of photoinhibition and with the relative independence of photoinhibition of PSII electron transfer reactions (Figs. 1 and 2), because the damage caused by Mn excitation is not expected to be influenced by non-photochemical or photochemical quenching. The small enhancement of photoinhibition by photochemical quenching reflects the role of $P_{680}^{+}$ in reactions occurring after damage to OEC. The similarity of the quantum yield of photoinhibition under various intensities of continuous light and Xenon flash illumination (Fig. 3) is also consistent with the fact that Mn absorption is directly proportional to the amount of light and not influenced by the rate of photosynthetic electron transfer. Thus, current data support the conclusion that a photoinhibition mechanism based on direct effect of light on the oxygen-evolving manganese cluster has significance under UV light, visible light and under illumination with short Xenon flashes.

## Acknowledgements

This work was financially supported by the Academy of Finland and Turku University Foundation.

## References

[1] O. Prasil, N. Adir, I. Ohad, Dynamics of photosystem II: mechanism of photoinhibition and recovery processes, in: J. Barber (Ed.), Topics in Photosynthesis, The Photosystems: Structure, Function and Molecular Biology, vol. 11, Elsevier, Amsterdam, 1992, pp. 293–348.
[2] E.-M. Aro, I. Virgin, B. Andersson, Photoinhibition of Photosystem II. Inactivation, protein damage and turnover, Biochim. Biophys. Acta 1143 (1993) 113–134.
[3] A. Melis, Photosystem-II damage and repair cycle in chloroplasts: what modulates the rate of photodamage? Trends Plant Sci. 4 (1999) 130–135.
[4] B. Andersson, E.-M. Aro, Photodamage and D1 protein turnover in Photosystem II, in: E.-M. Aro, B. Andersson (Eds.), Regulation of Photosynthesis, Kluwer Academic Publishers, Dordrecht, 2001, pp. 377–393.
[5] I. Vass, S. Styring, T. Hundal, A. Koivuniemi, E.-M. Aro, B. Andersson, Reversible and irreversible intermediates during photoinhibition of photosystem II. Stable reduced $Q_A$ species promote chlorophyll triplet formation, Proc. Natl. Acad. Sci. U. S. A. 89 (1992) 1408–1412.
[6] N. Keren, A. Berg, P.J.M. van Kan, H. Levanon, I. Ohad, Mechanism of photosystem II photoinactivation and D1 protein degradation at low light: the role of back electron flow, Proc. Natl. Acad. Sci. U. S. A. 94 (1997) 1579–1584.
[7] F.E. Callahan, D.W. Becker, G.M. Cheniae, Studies on the photoinactivation of the water-oxidizing enzyme. II. Characterization of weak light photoinhibition of PSII and its light-induced recovery, Plant Physiol. 82 (1986) 261–269.
[8] H.-J. Eckert, B. Geiken, J. Bernarding, A. Napiwotzki, H.-J. Eichler, G. Renger, Two sites of photoinhibition of the electron transfer in oxygen evolving and Tris-treated PSII membrane fragments from spinach, Photosynth. Res. 27 (1991) 97–108.
[9] G.-X. Chen, J. Kazimir, G.M. Cheniae, Photoinhibition of hydroxylamine-extracted photosystem II membranes: studies of the mechanism, Biochemistry 31 (1992) 11072–11083.
[10] J.M. Anderson, Y.-I. Park, W.S. Chow, Unifying model for the photoinactivation of photosystem II in vivo: a hypothesis, Photosynth. Res. 56 (1998) 1–13.
[11] J. Jung, H.-S. Kim, The chromatophores as endogenous sensitizers involved in the photogeneration of singlet oxygen in spinach thylakoids, Photochem. Photobiol. 52 (1990) 1003–1009.
[12] S. Santabarbara, K.V. Neverov, F.M. Garlaschi, G. Zucchelli, R.C. Jennings, Involvement of uncoupled antenna chlorophylls in photoinhibition in thylakoids, FEBS Lett. 491 (2001) 109–113.
[13] B.M. Greenberg, V. Gaba, O. Canaani, S. Malkin, A.K. Mattoo, M. Edelman, Separate photosensitizers mediate degradation of the 32-kDa photosystem II reaction center protein in the visible and UV spectral regions, Proc. Natl. Acad. Sci. U. S. A. 86 (1989) 6617–6662.
[14] R. Barbato, A. Frizzo, G. Friso, F. Rigoni, G.M. Giacometti, Degradation of the D1 protein of photosystem-II reaction centre by ultraviolet-B radiation requires the presence of functional manganese on the donor side, Eur. J. Biochem. 227 (1995) 723–729.
[15] L.W. Jones, B. Kok, Photoinhibition of chloroplast reactions. I. Kinetics and action spectra, Plant Physiol. 41 (1966) 1037–1043.
[16] E. Tyystjärvi, E.-M. Aro, The rate constant of photoinhibition, measured in lincomycin-treated leaves, is directly proportional to light intensity, Proc. Natl. Acad. Sci. U. S. A. 93 (1996) 2213–2218.
[17] B. Demmig-Adams, W.W. Adams, D.H. Barker, B.A. Logan, D.R. Bowling, A.S. Verhoeven, Using chlorophyll fluorescence to assess the fraction of absorbed light allocated to thermal dissipation of excess excitation, Physiol. Plant. 98 (1996) 253–264.
[18] H.-D. Brauer, R. Schmidt, G. Gauglitz, S. Hubig, Chemical actinometry in the visible (475–610 nm) by meso-diphenylhelianthrene, Photochem. Photobiol. 37 (1983) 595–598.
[19] D.V. Vavilin, E. Tyystjärvi, E.-M. Aro, Model for the fluorescence induction curve of photoinhibited thylakoids, Biophys. J. 75 (1998) 503–512.
[20] C.G. Hatchard, C.A. Parker, A new sensitive chemical actinometer: II. Potassium ferrioxalate as a standard chemical actinometer, Proc. R. Soc. Lond., A 295 (1956) 518–536.
[21] E. Pätsikkä, E.-M. Aro, E. Tyystjärvi, Increase in the quantum yield of photoinhibition contributes to copper toxicity in vivo, Plant Physiol. 117 (1998) 619–627.
[22] D.M. Stokes, D.A. Walker, Photosynthesis by isolated chloroplasts. Inhibition by DL-glyceraldehyde of carbon dioxide assimilation, Biochem. J. 128 (1972) 1147–1157.
[23] R. Hollinderbäumer, V. Ebbert, D. Godde, Inhibition of $CO_2$-fixation and its effect on the activity of Photosystem II, on D1-protein synthesis and phosphorylation, Photosynth. Res. 52 (1997) 105–116.
[24] C.W. Hoganson, G.T. Babcock, A metalloradical mechanism for the generation of oxygen from water in photosynthesis, Science 277 (1997) 1953–1956.
[25] D. Kuzek, R.J. Pace, Probing the Mn oxidation states in the OEC. Insights from spectroscopic, computational and kinetic data, Biochim. Biophys. Acta 1503 (2001) 123–137.
[26] M.E. Bodini, L.A. Willis, T.L. Riechel, D.T. Sawyer, Electrochemical and spectroscopic studies of manganese(II), -(III), and -(IV) gluconate complexes. 1. Formulas and oxidation–reduction stoichiometry, Inorg. Chem. 15 (1976) 1538–1543.
[27] J.P. Dekker, H.J. van Gorkom, M. Brock, L. Ouwehand, Optical characterization of photosystem II electron donors, Biochim. Biophys. Acta 764 (1984) 301–309.
[28] O. Horner, E. Anxolabéhère-Mallart, M.-F. Charlot, L. Tchertanov, J. Guilhem, T.A. Mattioli, A. Boussac, J.-J. Girerd, A new manganese dinuclear complex with phenolate ligands and a single unsupported oxo bridge. Storage of two positive charges within less than 500 mV. Relevance to photosynthesis, Inorg. Chem. 38 (1999) 1222–1232.

[29] C. Baffert, M.-N. Collomb, A. Deronzier, J. Pécaut, J. Limburg, R.H. Crabtree, G. Brudvig, Two new Terpyridine dimanganese complexes: a manganese(III,III) complex with a single unsupported oxo-bridge and a Manganese (III,IV) complex with a dioxo bridge. Synthesis, structure and redox properties, Inorg. Chem. 41 (2002) 1401–1411.
[30] I. Virgin, S. Styring, B. Andersson, Photosystem II disorganization and manganese release after photoinhibition of isolated spinach thylakoid membranes, FEBS Lett. 233 (1988) 408–412.
[31] N. Adir, H. Zer, S. Shochat, I. Ohad, Photoinhibition—historical perspective, Photosynth. Res. 76 (2003) 343–370.
[32] E. Tyystjärvi, N. King, M. Hakala, E.-M. Aro, Artificial quenchers of chlorophyll fluorescence do not protect against photoinhibition, J. Photochem. Photobiol., B Biol. 48 (1999) 142–147.
[33] S. Santabarbara, R. Barbato, G. Zucchelli, F.M. Garlaschi, R.C. Jennings, The quenching of photosystem II fluorescence does not protect the D1 protein against light induced degradation in thylakoids, FEBS Lett. 505 (2001) 159–162.
[34] M.C. Kato, K. Hikosaka, N. Hirotsu, A. Makino, T. Hirose, The excess light energy that is neither utilized in photosynthesis nor dissipated by photoprotective mechanisms determines the rate of photoinactivation in photosystem II, Plant Cell Physiol. 44 (2003) 318–325.
[35] T.D. Tsonev, K. Hikosaka, Contribution of photosynthetic electron transport, heat dissipation, and recovery of photoinactivated photosystem II to photoprotections at different temperatures in *Chenopodium album* leaves, Plant Cell Physiol. 44 (2003) 828–835.
[36] J. De Las Rivas, A. Telfer, J. Barber, Two coupled β-carotene molecules protect P680 from photodamage in isolated Photosystem II reaction centres, Biochim. Biophys. Acta 1142 (1993) 155–164.
[37] V. Hurry, J.M. Anderson, M.R. Badger, G.D. Price, Reduced levels of cytochrome *b*(6)*f* in transgenic tobacco increases the excitation pressure on Photosystem II without increasing sensitivity to photoinhibition in vivo, Photosynth. Res. 50 (1996) 159–169.
[38] A. Krieger-Liszkay, K. Kienzler, G.N. Johnson, Inhibition of electron transport at the cytochrome $b_6f$ complex protects photosystem II from photoinhibition, FEBS Lett. 486 (2000) 191–194.
[39] É. Hideg, C. Spetea, I. Vass, Singlet oxygen production in thylakoid membranes during photoinhibition as detected by EPR spectroscopy, Photosynth. Res. 39 (1994) 191–199.
[40] É. Hideg, T. Kálai, K. Hideg, I. Vass, Photoinhibition of photosynthesis in vivo results in singlet oxygen production detection via nitroxide-induced fluorescence quenching in broad bean leaves, Biochemistry 37 (1998) 11405–11411.
[41] S. Rinalducci, J.Z. Pedersen, L. Zolla, Formation of radicals from singlet oxygen produced during photoinhibition of isolated light-harvesting proteins of photosystem II, Biochim. Biophys. Acta 1608 (2004) 63–73.
[42] I. Vass, Z. Máté, E. Turcsányi, L. Sass, A. Szilárd, F. Nagy, C. Sicora, Damage and repair of photosystem II under exposure to UV radiation, Proceedings of the 12th International Congress on Photosynthesis, CSIRO Publishing, Brisbane, 2001, CD-ROM.
[43] A. Krieger, A.W. Rutherford, I. Vass, É. Hideg, Relationship between activity, D1 loss, and Mn binding in photoinhibition of photosystem II, Biochemistry 37 (1998) 16262–16269.
[44] T. Tyystjärvi, I. Tuominen, M. Herranen, E.-M. Aro, E. Tyystjärvi, Action spectrum of psbA gene transcription is similar to that of photoinhibition in *Synechocystis* sp. PCC 6803, FEBS Lett. 516 (2002) 167–171.
[45] J. Limburg, J.S. Vrettos, L.M. Liable-Sands, A.L. Rheingold, R.H. Crabtree, G.W. Brudvig, A functional model for O–O bond formation by the $O_2$-evolving complex in photosystem II, Science 283 (1999) 1524–1527.
[46] R.V. Bensasson, E.J. Land, T.G. Truscott, Flash Photolysis and Pulse Radiolysis, Pergamon Press, Oxford, 1983.